УДК 539.114

COLLECTIVE STATES IN ^{230}Th: EXPERIMENTAL DATA

A. I. Levon[1], G. Graw[2], Y. Eisermann[2], R. Hertenberger[2], P. G. Thirolf[2], H.-F. Wirth[2]

[1]*Institute for Nuclear Research, National Academy of Sciences of Ukraine, Kyiv*
[2]*Fakultat fur Physik, Ludwig-Maximilians-Universitat Munchen, Garching, Germany*

The excitation spectra in the deformed nucleus ^{230}Th were studied by means of the (p, t) reaction, using the Q3D spectrograph facility at the Munich Tandem accelerator. The angular distributions of tritons are measured for about 200 excitations seen in the triton spectra up to 3.3 MeV. Firm 0+ assignments are made for 16 excited states by comparison of experimental angular distributions with the calculated ones using the CHUCK3 code and relatively firm - for 4 states. Assignments up to spin 6^+ are made for other states. Analysis of the obtained data will be presented in forthcoming paper.

Keywords: (p, t)-spectroscopy, Q3D spectrograph, angular distributions, couple channel analysis, collective states.

Introduction

A full microscopic description of low-lying excitations in deformed nuclei has eluded theoretical studies to date. Along with the interplay of collective and single-particle excitations, which takes place in deformed rare earth nuclei, additional problems arise in the actinide region because of the reflection asymmetry [1]. Evidently the nature of the first excited 0^+ states in the actinide nuclei is different from that in the rare earth region where they are due to the quadrupole vibration [2]. Octupole degrees of freedom have to be important in the actinides. One has then to expect a complicated picture at higher excitations: residual interactions could mix the one-phonon and multiphonon vibrations of quadrupole and octupole character with each other and with quasiparticle excitations. Detailed experimental information on the properties of such excitations is needed for comparison with theory. On the experimental side, the (p, t) reaction is very useful. On the theoretical side, a microscopic approach such as the quasiparticle-phonon model (QPM) is necessary in order to account for the number of states detected and to make detailed predictions on their properties. The (p, t) reaction, however, gives much more extensive information on specific excitations in these nuclei, which was not analyzed previously in our paper [3]. In this paper we present the results of a careful and detailed analysis of the experimental data from the high-precision, high-resolution study of the ^{232}Th(p, t)^{230}Th reaction carried out to get deeper insight into excitations in ^{230}Th including the nature of the 0^+ excitations.

Experiment, analysis and experimental data

Details of the experiment

A target of 100 μg/cm^2 ^{232}Th evaporated on a 22 μg/cm^2 thick carbon backing was bombarded with 25 MeV protons of an intensity of 1 - 2 μA from the Tandem accelerator of the Maier - Leibnitz - Labor of the Ludwig - Maximilians - Universität and Technische Universität München. The isotopic purity of the target was about 99 %. The tritons were analyzed with the Q3D magnetic spectrograph and then detected in a focal plane detector. The focal plane detector is a multiwire proportional chamber with readout of a cathode foil structure for position determination and dE/E particle identification [4, 5]. The acceptance of the spectrograph was 11 msr, except for the most forward angle of 5° with an acceptance of 6 msr. The resulting triton spectra have a resolution of 4 - 7 keV (FWHM) and are background free for all angles but 5° for which background from light contaminations in the region of 1100 - 1150 keV complicated the analysis for some levels. The angular distributions of the cross sections were obtained from the triton spectra at ten laboratory angles from 5 to 45°.

A triton energy spectrum measured at a detection angle of 7.5° is shown in Fig. 1, which demonstrates the domination of 0^+ excitations having large cross sections at this angle. The analysis of the triton spectra was performed with the program GASPAN [6]. Measurements were carried out with two magnetic settings: one for excitations up to 1.6 MeV and another for the energy region from 1.5 to 3.3 MeV. For the calibration of the energy scale the triton spectra from the reaction ^{184}W(p, t)^{182}W, ^{186}W(p, t)^{184}W and ^{234}U(p, t)^{232}U were measured at the same magnetic settings.

About 200 levels have been identified in the spectra for all ten angles and are listed in Table 1. The energies and spins of the levels as derived from this study are compared to known energies and spins from the published data [7, 8]. They are given in the first four columns. The ratios of cross sections at angles 5 and 26° to that at angle 16°, given in the next two columns, help to highlight the 0+ excitations (large values). The column $\sigma_{integ.}$ gives

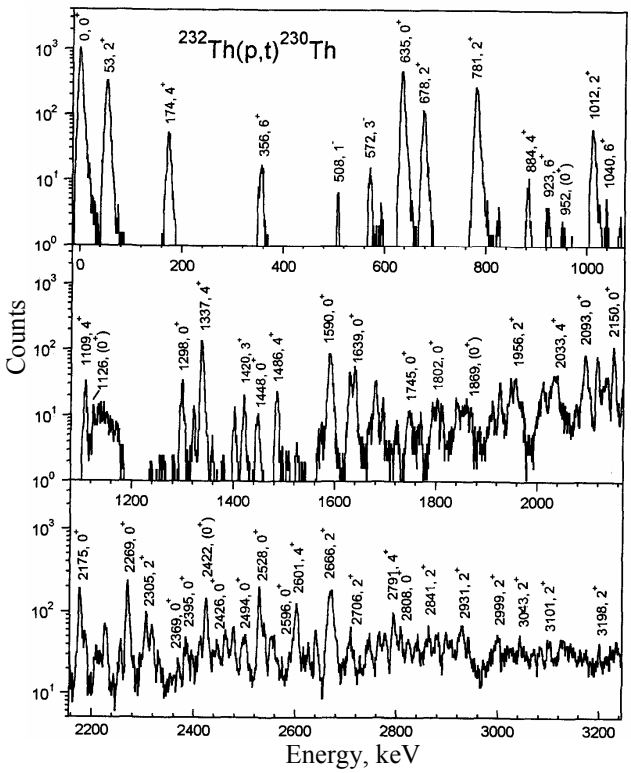

Fig. 1. Triton energy spectrum from the ^{232}Th(p, t)^{230}Th reaction (E_p = 25 MeV) in logarithmic scale for a detection angle of 7.5°. Some strong lines are labeled with the corresponding level energies in keV and by the spins assigned from the DWBA fit.

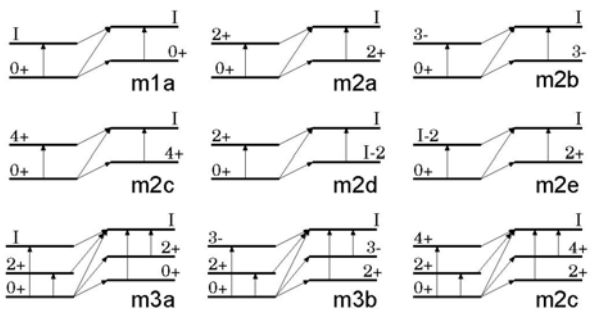

Fig. 2. Schemes of the CHUCK3 multi-step calculations tested with spin assignments of excited states in ^{230}Th (see Table I).

the cross section integrated in the region from 5 to 45° and the column $\sigma_{exp.}/\sigma_{calc.}$ gives the ratio of the integrated cross sections, from experimental values and calculations in the DWBA approximation. The last column gives the notations of the schemes used in the DWBA calculations: sw.jj means one-step direct transfer of the $(j)^2$ neutrons in the (p, t) reaction; notations of the multi-way transfers used in the DWBA calculations are displayed in Fig. 2.

Table 1. **Energies of levels in ^{230}Th, the level spin assignments from the CHUCK3 analysis, the (p, t) cross sections integrated over the measured values and the reference to the schemes used in the DWBA calculations (see text for more detailed explanations)**

Level energy, keV		I^π		Cross section ratios		$\sigma_{integ.}$, μb	Ratio	Way of fitting
This work	[7 - 8]	[7 - 8]	This work	(5°/16°)	(26°/16°)		$\sigma_{exp.}/\sigma_{calc.}$	
0.1 (2)	0.0	0^+	0^+	8.02	5.51	195.68	10.7	sw.gg
53.2 (2)	53.20 (2)	2^+	2^+	1.57	0.27	52.53	11.0	mla
174.0 (2)	174.10 (3)	4^+	4^+	0.87	0.50	9.94	2.6	mla
356.3 (2)	356.6 (5)	6^+	6^+	0.40	0.75	7.39	2.8	m2d
508.0 (3)	508.15 (3)	1^-	1^-	0.63	0.00	0.87	0.6	m2a
571.7 (2)	571.73 (3)	3^-	3^-	0.33	0.44	4.04	0.8	m3a
593.8 (3)	594.1 (5)	8^+	8^+	1.05	0.00	0.37	0.4	m2c
635.1 (2)	634.88 (5)	0^+	0^+	26.91	8.92	47.79	250	sw.ii
677.6 (2)	677.54 (5)	2^+	2^+	0.85	0.55	25.13	3.5	mla
686.0 (10)	686.7	5^-				< 0.2		
775.2 (4)	775.5 (3)	4^+	4^+	0.30	0.53	7.15	1.3	mla
781.4 (2)	781.35 (3)	2^+	2^+	0.62	0.46	69.07	6.2	sw.gg
825.6 (3)	825.66 (5)	3^+	3^+	0.14	0.79	1.10	2.5	m2a
852.7 (4)	851.88 (3)	7^-				0.42		
884.2 (4)	883.9 (2)	4^+	4^+	0.51	1.27	4.09	0.8	mla
923.3 (5)	923.0 (2)	6^+	6^+	1.66	0.96	0.50	0.2	m2d
952.6 (5)	951.88 (5)	1^-	1^-	1.17	1.76	0.71	0.03	m1a[a]
			or (0^+)				0.6	sw.ij[a]
	955.1 (2)	5+						
972.1 (5)	971.72 (5)	2-	2-	0.22	0.69	0.37	5.0	m2a
1011.6 (5)	1009.58 (5)	2+	2+	0.54	0.34	14.34	2.1	sw.gg
	1012.51 (5)	3-	3-				6.0	sw.gg
1040.0 (7)	1039.6 (2)	6+	6+	0.80	1.07	0.94	0.5	m2a
1052.0 (7)	1052.31 (5)	3+	3+	0.00	3.33	0.34	0.8	m2a
1065.9 (8)			4-	0.99	0.69	0.30	0.45	m3b
1079.4 (8)	1079.21 (3)	2-	2-	0.00	0.00	0.09	0.1	m3b

Continuation of the Table 1

Level energy, keV		I^{π}		Cross section ratios		$\sigma_{integ.}$, μb	Ratio	Way of fitting
This work	[7 - 8]	[7 - 8]	This work	(5°/16°)	(26°/16°)		$\sigma_{exp.}/\sigma_{calc.}$	
1108.7 (5)	1107.5 (3)	4^+	4^+	1.20	0.87	5.38	1.2	m2a
	1109.0 (1)	5^-						
	1117.5 (3)	8^+						
1125.6 (5)			(1^-)	4.54	1.06	2.10	0.1	m1a[a]
			or (0^+)				1.5	sw.jj[a]
	1127.76 (5)	3^-						
	1134.4 (2)	7^+						
1148.0 (9)						<0.2		
	1176.1 (3)	5^+						
1184.8 (9)						<0.2		
	1196.8	(4^-)						
1241.2 (9)	1243.3 (3)	8^+				<0.2		
1256.0 (9)	1255.5 (3)	6^+				<0.2		
1259.2 (6)			(3^-)	0.97	0.34	0.34	0.3	sw.gg
1283.6 (6)			(5^-)	1.08	0.00	0.23	0.07	m3b
1297.8 (6)	1297.1 (1)	0^+	0^+	4.37	2.53	4.15	1.8	sw.ig
1322.3 (5)			(3^-)	1.23	0.54	1.77	1.5	sw.gg
1337.2 (5)			4^+	1.37	1.14	24.42	3.2	sw.gg
	1349.3 (4)	7^+						
1359.5 (7)			(2^+)	0.00	0.41	0.48	0.05	sw.gg
1376.6 (7)	1375.3 (1)	1,2+	$1^+,5^-$	0.00	0.00	0.24	0.2/0.1	m3b
1401.5 (5)	1400.9 (1)	2^+	2^+	0.49	0.38	3.18	0.3	sw.gg
1420.4 (5)			(3^+)	0.33	0.70	4.74	1.0	m2a
1440.4 (8)			(3^+)			<0.2		
1447.9 (5)			0^+	10.37	6.86	1.70	0.05	sw.gg
1485.6 (5)	1485.6 (1)		4^+	1.44	0.93	4.59	0.6	sw.gg
1496.0 (10)						<0.2		
1507.4 (5)			4+	1.29	2.28	0.57	0.07	m2a
1524.8 (5)			2+	0.66	0.00	0.53	0.05	sw.gg
1566.2 (6)			(1-)	1.80	0.29	0.31	0.15	m2b
1574.5 (6)	1573.5 (2)	1(-), 2+	(2-)	0.34	0.70	2.14	3.8	m2a
1584.7 (6)			(4-, 5+)	1.77	1.90	2.64	42/36	m2a
1590.2 (5)	1589.8 (2)	0+	0+	8.48	6.04	11.66	0.28	sw.gg
1594.7 (8)			(1-)	1.11	0.58	2.22	1.5	m3b
1601.2 (11)			(3-)	1.46	1.14	0.74	0.8	sw.gg
1612.1 (10)			(4-, 5+)	1.26	2.25	0.36	8.3/1	m2a
1618.7 (9)			(4-, 5+)	1.44	2.09	0.27	8.0/0.9	m2a
1630.1 (7)	1628 (2)		2+	1.43	0.45	4.49	0.6	mla
1639.3 (6)	1638.5 (2)	(2,0+)	0+	5.68	4.64	8.32	0.2	sw.gg
1653.2 (11)			(6+)	0.96	1.75	0.88	0.004	m3a
1668.2 (7)			4+	1.54	1.85	1.91	0.3	sw.gg
1679.1 (7)			2+	1.72	0.36	3.36	0.45	mla
1683.3 (7)			(4-)	0.19	1.95	2.20	34	m2a
1694.9 (7)	1695.7 (1)	1(-), 2+	(4+)	1.09	1.41	3.57	0.35	sw.gg
1708.8 (8)			2+	0.22	0.18	0.38	0.03	sw.gg
1723.5 (7)			(4+)	0.55	1.35	2.31	0.3	mla
1745.3 (8)	1744.9 (1)		0+	2.80	2.59	1.18	0.10	sw.jg
1750.7 (8)			(3-)	1.76	0.64	0.99	0.8	sw.gg
1762.3 (8)			(4+)	0.73	0.43	0.89	0.2	mla
1769.6 (8)	1770.7 (1)	1,2+	(4+)	0.52	0.69	0.89	0.15	sw.gg
1774.1 (9)	1775.2 (1)	1,2+				<0.2		
	1789.4 (5)	1(-), 2+						
1793.1 (6)			(5-)	1.19	1.19	2.43	3.5	sw.gg
1802.5 (6)			0+	8.04	5.38	2.38	0.05	
	1810.7 (1)	1,2+						
1812.0 (8)			4+	1.71	0.96	1.26	0.13	sw.gg
1824.9 (7)			(6+)	0.45	0.96	1.15	0.15	sw.gg
1840.0 (8)	1839.6 (2)	1(-), 2+	2+	1.74	0.70	2.37	0.25	mla
1851.4 (7)	1849.6 (1)	(2+)	(3-)	1.07	0.93	1.73	1.5	sw.gg
1859.3 (7)	1858.2 (6)		(3-)	1.41	1.05	1.74	1.6	sw.gg
1868.9 (7)			(0+)	1.99	1.60	1.73	0.03	sw.ggb

Continuation of the Table 1

Level energy, keV		I^{π}		Cross section ratios		$\sigma_{integ.}$, μb	Ratio	Way of fitting
This work	[7 - 8]	[7 - 8]	This work	(5°/16°)	(26°/16°)		$\sigma_{exp}/\sigma_{calc.}$	
			+(6+)				0.26	m2db
1887.0 (9)			(2^+)	0.84	0.68	0.76	0.06	sw.gg
	1902.7 (1)	$1,2^+$						
1910.0 (9)			(6^+)	0.51	1.13	1.84	0.25	sw.gg
1914.7 (9)			(1^-)	0.91	0.57	1.18	0.8	m2a
1926.0 (7)			4^+	2.18	0.90	1.71	0.6	m2a
1931.1 (8)			(1^-)	0.81	0.50	0.62	0.5	m2a
1939.8 (11)			$(1^-,1^+)$	0.36	0.68	0.98	0.6	m2a
1947.0 (6)			4^+	1.18	0.89	3.81	0.4	mla
	1949.8 (1)	$1,2^+$						
1956.4 (6)			2^+	0.39	0.47	6.96	0.35	sw.gg
1967.1 (7)	1966.9 (2)	$1,2^+$	2^+	0.27	0.66	3.76	0.18	sw.gg
1972.0 (9)	1973.4 (2)	$(1^+,2^+)$	2^+	0.58	0.39	0.94	0.05	sw.gg
1985.4 (8)			(5^-)	0.00	0.52	0.51	0.8	sw.gg
2001.6 (8)	2000.9 (1)	$1,2^+$	(3^-)	1.28	0.83	1.15	1.1	sw.gg
2010.3 (6)	2010.1 (2)	$1,2^+$	2^+	0.26	0.38	5.69	0.3	sw.gg
2017.3 (7)			(3^-)	1.03	0.73	1.75	1.6	sw.gg
2025.6 (6)	2024.7 (2)	$1^+,2^+$	2^+	0.28	0.39	3.84	0.2	sw.gg
2032.8 (7)			4^+	1.07	1.13	5.69	0.5	sw.gg
2039.1 (7)			4^+	2.24	1.85	4.51	0.4	sw.gg
2048.7 (7)			(4^+)	1.00	1.19	1.59	0.15	sw.gg
2060.9 (12)			(3^-)	2.05	0.55	0.87	0.02	m3a
2073.2 (8)			(8^+)	0.00	1.82	1.40	0.4	sw.gg
2074.9 (8)			(4^+)	0.85	0.51	1.16	0.2	m1a
2085.9 (8)			(4^+)	1.75	1.26	1.60	0.15	sw.gg
2093.9 (7)			0^+	4.44	2.17	6.93	13	sw.ii
2102.0 (7)			4^+	2.30	1.10	1.26	0.15	sw.gg
2118.4 (6)			4^+	2.32	1.14	7.70	0.90	sw.gg
	2122.8 (1)	$1,2^+$						
2130.7 (7)			2^+	0.51	0.76	5.23	0.2	sw.gg
	2133.2 (2)							
2137.9 (7)			2^+	0.51	0.50	4.87	0.2	sw.gg
2150.5 (6)			0+	10.53	3.87	6.57	25	sw.ii
	2151.8 (2)	$1,2^+$						
2168.8 (7)			(4^+)	1.12	1.37	2.31	0.2	sw.gg
2175.1 (6)			0^+	21.75	8.97	11.93	42	sw.ii
2181.7 (7)			(4^+)	1.02	2.07	4.22	0.35	sw.gg
2187.1 (6)			2^+	0.39	0.57	8.14	0.30	sw.gg
2194.8 (8)			(6^+)			0.59	0.25	m2a
2205.4 (10)			2^+	0.49	0.47	2.67	0.10	sw.gg
2207.8 (8)			(4^+)	1.99	2.40	2.74	0.2	sw.gg
2216.0 (7)			(4^+)	1.07	0.44	1.62	0.4	m2a
2226.0 (6)			2^+	0.56	0.54	9.84	0.5	sw.gg
2241.0 (7)			2^+	0.29	0.49	1.13	0.06	sw.gg
2249.9 (7)			(6^+)	0.46	1.22	1.54	0.2	sw.gg
2255.3 (7)			4^+	1.81	1.41	3.79	0.4	sw.gg
2268.9 (6)			0^+	15.37	6.16	14.86	56	sw.ii
2276.0 (8)			(4^+)	0.00	2.02	1.59	0.15	sw.gg
2282.1 (10)	2282.8 (5)	$1,2^+$						
2295.9 (8)			4+	3.08	1.78	2.20	0.25	sw.gg
	2298.6 (3)	$1,2^+$						
2305.4 (7)			2^+	0.52	0.53	13.62	0.7	sw.gg
2311.2 (8)			(4^+)	0.41	1.20	2.33	0.2	sw.gg
	2314.3 (2)	$1,2^+$						
2317.7 (7)			4^+	2.75	1.27	4.95	0.5	sw.gg
2329.6 (7)			2^+	0.37	0.34	2.65	0.1	sw.gg
2337.1 (8)			(5^-)	0.90	0.87	1.28	2.0	sw.gg
2354.8 (10)			(6^+)	2.12	2.20	0.60	1.6	m2a
2368.5 (7)	2368.9 (2)		(0^+)	2.75	3.79	1.70	0.23	sw.jg
2383.8 (8)			(4^+)	1.02	0.87	4.54	0.3	m2a
2388.4 (10)						1.32		

Continuation of the Table 1

Level energy, keV		I^{π}		Cross section ratios		$\sigma_{integ.}$, μb	Ratio	Way of fitting
This work	[7 - 8]	[7 - 8]	This work	(5°/16°)	(26°/16°)		$\sigma_{exp.}/\sigma_{calc.}$	
2395.2 (7)			0^+	3.95	2.14	0.94	2.8	sw.ii
2422.7 (7)			(4^+)	3.20	1.87	8.3	0.8	sw.gg[b]
			$+(0^+)$			5.2	7.5	sw.ii[b]
2426.4 (9)			(0^+)	3.11	2.30	3.50	6.7	sw.ii
2436.6 (9)			2^+	0.33	0.49	2.20	0.10	sw.gg
2442.5 (8)			2^+	0.65	0.68	3.73	0.15	sw.gg
2449.2 (2)			(3^-)	1.34	0.71	1.65	1.6	sw.gg
2461.0 (7)			2^+	0.41	0.62	8.08	0.4	sw.gg
2467.2 (7)			$2^+,3^-$	0.49	0.79	3.55	0.15	sw.gg
2474.3 (8)			2^+	0.15	0.50	5.20	0.25	sw.gg
2478.5 (8)			4^+	2.20	1.00	5.00	0.5	sw.gg
2481.3 (12)			(6^+)	0.03	0.16	1.21	0.5	m2a
2493.8 (7)			0^+	5.62	3.92	3.40	1.4	sw.ig
2501.1 (7)			4^+	1.43	1.41	4.70	0.6	sw.gg
2508.3 (7)				0.00	1.68	0.76		
2519.3 (7)			(6^+)	0.00	1.13	1.43	0.5	m2a
2528.1 (7)			0^+	11.96	6.76	12.36	5.6	sw.ig
2536.9 (7)			4^+	1.36	1.43	6.07	0.6	sw.gg
2549.8 (11)			0^+	4.32	2.60	2.75	1.2	sw.ig
2556.2 (8)			(4^+)	0.85	1.10	4.05	0.75	m1a
2562.9 (9)			(4^+)	0.00	0.83	1.56	0.2	sw.gg
2573.2 (7)			(6^+)	0.00	1.18	1.33	0.5	m2a
2589.1 (7)			2^+	0.49	0.64	3.92	0.15	sw.gg
2596.4 (8)			(0^+)	31.20	10.35	2.50	5.1	sw.ii
2601.3 (7)			(4^+)	1.34	0.93	14.48	2.8	m2a
2616.0 (7)			2^+	0.55	0.61	2.76	0.4	sw.gg
2625.9 (7)			2^+	0.37	0.40	4.41	0.15	sw.gg
2640.0 (8)			4^+	1.83	1.55	7.41	0.7	sw.gg
2660.9 (7)			4^+	2.92	2.29	4.24	0.3	sw.gg
2666.4 (7)			(2^+)	0.34	0.58	26.48	1.5	sw.gg
2671.6 (7)			4^+	1.77	1.07	11.82	1.2	sw.gg
2679.2 (8)			2^+	0.39	0.30	3.77	0.15	sw.gg
2694.9 (7)			2^+	0.49	0.43	1.25	0.06	sw.gg
2706.5 (7)			2^+	0.79	0.53	6.14	0.2	sw.gg
2712.9 (8)			(6^+)	0.74	1.17	2.84	1.0	m2a
2726.6 (7)			2^+	1.02	0.87	2.28	0.1	sw.gg
2740.6 (7)			2^+	0.33	0.41	5.13	0.15	sw.gg
2746.2 (7)			4^+	3.35	1.84	2.77	0.3	sw.gg
2754.2 (10)			(6^+)	1.47	1.19	1.26	0.2	sw.gg
2764.9 (7)			2^+	0.66	0.70	8.03	0.3	sw.gg
2777.3 (7)			2^+	0.78	0.51	7.89	0.3	sw.gg
2791.5 (7)			4^+	1.77	1.09	11.49	1.2	sw.gg
2799.7 (8)			2^+	0.25	0.51	3.01	0.1	sw.gg
2808.1 (7)			0^+	7.72	3.30	4.86	8.5	sw.ii
2824.4 (10)			4^+	2.63	1.35	3.03	0.4	sw.gg
2834.0 (10)			2^+	0.18	0.69	2.58	0.2	sw.gg
2841.3 (7)			(2^+)	0.54	0.97	4.26	0.3	sw.gg
2855.9 (7)			2^+	0.51	0.82	4.04	0.3	sw.gg
2862.9 (7)			2^+	0.58	0.74	6.25	0.4	sw.gg
2870.6 (10)			(3^-)	1.50	0.93	1.26	1.2	sw.gg
2879.7 (7)			2+	0.76	0.62	5.49	0.5	sw.gg
2886.1 (10)			(1^-)	1.71	0.49	0.99	0.8	m2a
2896.1 (7)			2+	0.32	0.51	5.52	0.5	sw.gg
2906.4 (8)			(3^-)	0.75	1.07	3.42	2.6	sw.gg
2913.6 (15)			(4^+)	0.51	0.37	1.60	0.12	sw.gg
2923.7 (9)			2^+	0.51	0.85	5.87	0.4	sw.gg
2930.6 (7)			2^+	0.49	0.50	6.31	0.26	sw.gg
2940.6 (7)			2^+	0.37	0.53	3.84	0.3	sw.gg
2950.5 (8)			(6^+)	0.20	1.41	0.99	0.5	m2a
2987.9 (10)			(6^+)	0.49	0.96	3.75	0.6	sw.gg
2999.0 (7)			2+	0.46	0.71	7.66	0.6	sw.gg
3009.9 (8)			2+	0.34	0.67	2.78	0.2	sw.gg

Continuation of the Table 1

Level energy, keV		I^{π}		Cross section ratios		$\sigma_{integ.}$, μb	Ratio	Way of fitting
This work	[7 - 8]	[7 - 8]	This work	(5°/16°)	(26°/16°)		$\sigma_{exp.}/\sigma_{calc.}$	
3020.6 (8)			2^+	0.38	0.52	3.72	0.3	sw.gg
3030.3 (9)			2^+	0.40	0.95	3.83	0.3	sw.gg
3043.0 (7)			2^+	0.46	0.61	5.91	0.4	sw.gg
3052.4 (9)			(3^+)	0.51	1.08	3.53	4.2	m2a
3064.3 (15)			(2^+)	0.48	0.64	2.51	0.1	sw.gg
3072.6 (8)			(6^+)	0.64	1.20	3.82	0.5	sw.gg
3083.8 (7)			2^+	0.36	0.64	5.46	0.35	sw.gg
3100.9 (7)			2^+	0.41	0.58	6.07	0.40	sw.gg
3113.9 (12)			(<=4)	1.04	1.48	2.57		
3124.7 (8)			(4^+)	0.89	1.15	6.01	1.8	sw.gg
3135.9 (10)			(<=4)	1.42	1.10	4.52	0.7	sw.gg
3147.4 (8)			(<=4)	1.06	0.81	4.65		
3162.0 (7)			2^+	0.41	0.79	3.44	0.25	sw.gg
3173.6 (8)			2^+	0.27	0.63	3.29	0.25	sw.gg
3186.1 (7)			(6^+)	0.46	0.82	2.54	0.4	sw.gg
3198.4 (7)			2^+	0.63	0.72	3.56	0.1	sw.gg
3212.2 (7)			2^+	0.50	0.73	2.75	0.08	sw.gg
3223.1 (7)			2^+	0.54	0.79	3.14	0.08	sw.gg
3234.0 (7)				0.98	0.89	4.72		
3248.6 (7)			2^+	0.54	0.72	4.46	0.12	sw.gg
3258.8 (8)				1.38	1.33	5.09		
3269.9 (12)			(2^+)	0.85	0.83	4.29	0.12	sw.gg

[a] For levels at 952.6 and 1125.6 keV the angular distributions can be fitted by the DWBA calculations as spin 1^- or spin 0^+.
[b] For the levels at 1868.9 and 2422.7 keV the angular distributions are fitted by the DWBA calculations as doublet lines.

DWBA analysis

The spins of the excited states in the final nucleus ^{230}Th were assigned via an analysis of the angular distributions of tritons from the (p, t) reaction. In a previous publication [3] the angular distributions for 0^+ excitations were demonstrated to have a steeply rising cross section at very small reaction angles and a sharp minimum at a detection angle of about 14°. The angular distribution for the 0^+ ground state of ^{230}Th has such a shape. This pronounced feature helped us to identify these states in complicated and dense spectra without fitting experimental angular distributions. No complication of the angular distributions was expected, since the excitation of 0^+ states predominantly is a one-step process. This is not the case for the excitation of states with other spins, where multi-step processes could play a very important role.

The identification of other states is possible by fitting the experimental angular distributions with those calculated in the distorted-wave Born approximation (DWBA). A problem arising in such calculations is that we have no prior knowledge of the microscopic structure of these states. We can assume, however, that the overall shape of the angular distribution of the cross section is rather independent of the specific structure of the individual states, since the wave function of the outgoing tritons is restricted to the nuclear exterior and therefore to the tails of the triton form factors. The coupled channel approximation (CHUCK3 code of Kunz [9]) was used in these calculations.

The shape of the calculated angular distributions depends strongly on the chosen potential parameters. We used parameters suggested by Becchetti and Greenlees [10] for protons and by Flynn et al. [11] for tritons (Table 2). For each state the binding energies of the two neutrons are calculated to match the outgoing triton energies. The corrections to the reaction energy are introduced depending on the excitation energy. The best reproduction of the angular distribution for the ground state was obtained for the transfer of the $(2g_{9/2})^2$ configuration in the one-step process. This orbital is close to the Fermi surface and was considered as the most probable in the transfer process. Other transfer configurations that might be of importance are $(1i_{11/2})^2$ and $(1j_{15/2})^2$, since these orbitals are also near the Fermi surface. The shape of the angular distributions depends to some degree on the transfer configuration, the most pronounced being found for the 0^+ states. However, the main features of the angular distribution shapes for 2^+ and 4^+ states are not dependent on the transfer configurations. Therefore the $(2g_{9/2})^2$ configuration was used in the calculations for the majority of excited states.

Results of fitting the angular distributions for the states assigned as 0^+ excitations are shown in Fig. 3. The angular distributions in the two first columns

Table 2. **Optical potential parameters used in the DWBA calculations**

Parameters		p	t[a]	n	t[b]
V_r	(MeV)	57.10	166.70		159.0
$4W_D$	(MeV)	32.46			
W_0	(MeV)	2.80	10.28		9.24
$4V_{so}$	(MeV)	24.80			
r_r	(fm)	1.17	1.16	1.17	1.16
r_D	(fm)	1.32			
r_0	(fm)	1.32	1.50		1.50
r_{so}	(fm)	1.01			
R_c	(fm)	1.30	1.30		1.25
a_r	(fm)	0.75	0.75		0.75
a_D	(fm)	0.51			
a_0	(fm)	0.51	0.82		0.82
aso	(fm)	0.75			
nls		0.85	0.25		0.25

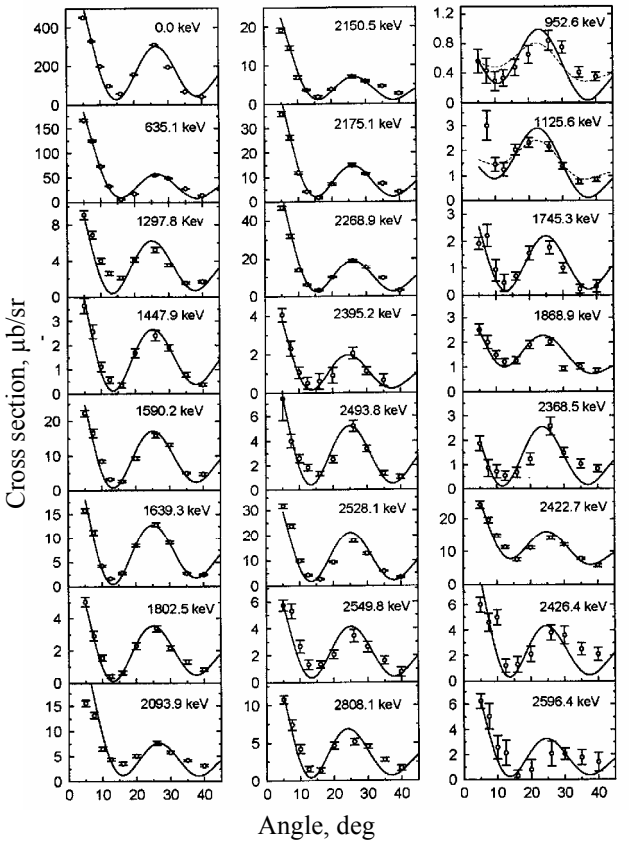

Fig. 3. Angular distributions of assigned 0^+ states in ^{230}Th and their fit with CHUCK3 one-step calculations. The (*ij*) transfer configurations used in the calculations for the best fit are given in Table 1. The first two columns on the left correspond to firm assignments and the column on the right to tentative assignments.

measured with good statistical accuracy are believed to give firm 0^+ assignments. Three possible transfer configurations $(2g_{9/2})^2$, $(1i_{11/2})^2$ and $(1j_{15/2})^2$ have been used to get the best fit to the experimental data. These configurations are listed in the last column in Table 1. The assignments to the states of 1745.3, 2368.5 2426.4 and 2596.4 keV are considered as relatively firm, because the shape of the angular distribution is fitted perfectly by the calculations although there is a limited statistical accuracy of the experimental data. The angular distribution for the transition at the excitation energy 1868.9 keV is fitted as a sum of two angular distributions for transfer to a 0^+ and a 6^+ state (doublet line). A similar situation is assumed for the energy 2422.7 keV, i.e. a superposition of two angular distributions for 0^+ and 4^+ states. In both cases assignments are tentative.

The angular distributions for the energies 952.6 and 1125.6 keV are a special case. A state with spin 1^- is known at the energy 951.9 keV, however the angular distribution of the tritons at an excitation energy of 952.6 keV is completely different from that for a known 1^- state at 508.1 keV. Nevertheless, it can by fitted satisfactorily by an inclusion of one-step and two-step excitations. At the same time this angular distribution can also be fitted by a calculation for a 0^+ excitation mainly by the $(1j_{15/2})^2$ transfer configuration with a small admixture of the $(1i_{11/2})^2$ transfer. A spin of 0+ is assigned to the state with closely lying energy of 927.3 keV in ^{232}U, studied in the alpha decay of ^{236}Pu [13]. Therefore, we have not excluded spin assignment 0+, though the present information is not sufficient to solve the problem. A similar angular distribution is observed for the excitation at 1125.6 keV. But in this case the known level at the closely lying energy of 1127.8 keV has spin of 3^-. The CHUCK calculations give a satisfactory fit for excitations of the 1^- and 0^+ states but not for 3^- state. Thus we can make firm spin assignments for 16 states, relatively firm assignments for 4 states and tentative assignments for 4 states, in comparison with 14 states found in the preliminary analysis of the experimental data [3].

Similar to 0+ excitations, the one-step transfer calculations give a satisfactory fit of angular distributions for about 70 % of the states with spins different from 0^+ but about 30 % of these states need the inclusion of multi-step excitations. Multi-step excitations have to be included to fit the angular distributions already for the 2^+, 4^+ and 6^+ states of the ground state band. Fig. 3 shows the schemes of the multi-step excitations tested for every state in those cases where one-step transfer does not provide a successful fit. Fig. 4 demonstrates the quality of the fit of some different-shaped angular distributions for the excitation of states with spins higher than 0^+ by calculations assuming one-step and one-step plus two-step excitations. Whereas natural parity states can be populated by one-step or one-step plus two-step mechanisms, the states of unnatural parity can be excited only by two-step excitations.

The assignments of the spins resulting from such fits are presented in Table 1 together with other

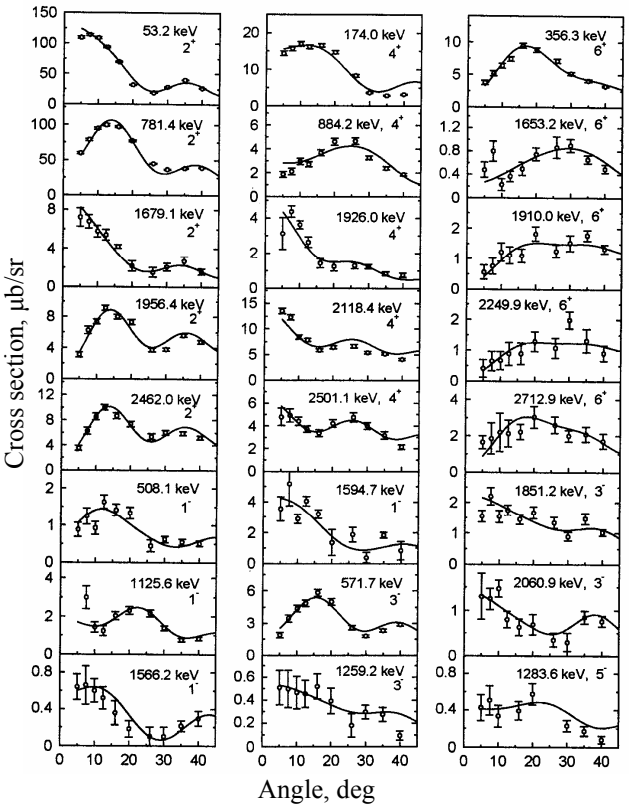

Fig. 4. Angular distributions of some excited states of natural parity and their fit by the CHUCK3 calculations. The (*ij*) transfer configurations and schemes used in the calculations for the best fit are given in Table 1.

experimental data. Special comments are needed for the column displaying the ratio $\sigma_{exp}/\sigma_{cal}$. Since we have no a priori knowledge of microscopic structure of the excited states and thus we do not know the relative contributions of the specific $(j)^2$ transfer configurations to each of these states, these ratios cannot be considered as spectroscopic factors. Nevertheless, a very large ratio, such as in the case of the $(1i_{11/2})^2$ transfer configurations used in the calculation for the 0^+ state at 635 keV, is unexpected. There are some contradictions in the assignment of the energy of the second 4^+ level. It has been proposed from Coulomb excitation to be at 772.1 keV in [14] and at 769.6 keV in [15] and from the (d, pnγ) reaction at 775.5 keV [8]. The value 769.6 keV is accepted in the compilation [7]. We see a weak peak at 775.2 keV on the tail of the very strong peak at 781.4 keV as confirmation of the 775.5 keV assignment [8]. There is not even a hint of a peak at 769.6 keV. Again the 8^+ and 10^+ levels proposed in [15] at 1251.4 keV and 1520.4 keV (both accepted in the compilation [7]) are in contradiction with the assignment of the 8^+ level at 1243.2 keV and with the calculated energy of the 10^+ level at 1487 keV [8]. The (p, t) study confirms the assignment for the 8^+ level at 1243.2 keV by the observation of a weak peak at 1241.2 keV and no peak in the vicinity of 1251.4 keV. After this confirmation the smooth change of the inertial parameter in the band prefers the energy 1487 keV for the 10^+ level and rejects the energy of 1520.4 keV.

There are several levels in ^{230}Th for which spins $1^{(-)}$, 2^+ or 1, 2^+ were assigned from the β^--decay and/or inelastic scattering and for which the (p, t) angular distributions are measured: 1573.5, 1695.7, 1770.7, 1839.6, 1849.6, 1966.9, 1973.4, 2000.9, 2010.1 and 2024.7 keV (energies are from the compilation [7]). Angular distributions from the (p, t) reaction confirm spin 2^+ for some of them: 1840.0, 1967.1, 1972.0, 2010.3 and 2025.6 keV (energies as determined from the (p, t) reaction). The (p, t) angular distributions for other states cannot be fitted for the spins given in [7]. If the energies 1574.5(6) keV from the (p, t) reaction and 1573.5(2) keV from [7] correspond to the same level, then a different assignment is suggested by the (p, t) angular distribution to this state as 2^- or 3^+. In any case a 2^+ excitation would manifest itself in the (p, t) angular distribution and therefore has to be excluded. For the states at 1694.9 and 1769.6 keV we observe angular distributions which can be fitted by calculations for 4^+ states (or even for a 0^+ state plus a constant of about 2 μb for the state of 1694.9 keV). Either way, the assignment 2^+ can be excluded. Finally, the (p, t) angular distributions for the states at 1851.4 and 2001.6 keV prefer an assignment of 3^- in contradiction to (2^+) and 1, 2^+, respectively, as given in [7]. Discussion of obtained experimental results will be presented in forthcoming paper.

Conclusion

Exited states in ^{230}Th have been studied in the (p, t) transfer reaction. About 200 levels were assigned using a DWBA fit procedure. Among them, 24 exited 0^+ states have been found in this nucleus, most of them have not been experimentally observed previously. Their accumulated strength makes up more than 70 % of the ground state strength. Firm assignments have been made for most of the 2^+ and 4^+ states and for some of the 6^+ states. The experimental data obtained in this study will be discussed in forthcoming paper.

REFERENCES

1. *Butler P. A., Nazarewicz W.* Intrinsic reflection asymmetry in atomic nuclei // Rev. Mod. Phys. - 1996. - Vol. 69, Issue 2. - P. 349 - 421.
2. *Maher J. V., Erskine J. R., Friedman A. M. et al.* Population of 0^+ States in Actinide and $A\approx190$ Nuclides by the (p, t) Reaction // Phys. Rev. - 1972. - Vol. C 5. - P. 1380 - 1389.
3. *Wirth H.-F., Graw G., Christen S. et al.* 0^+ states in deformed actinide nuclei by the (p, t) reaction // Phys. Rev. - 2004. - Vol. C 69, Issue 4. - P. 044310 - 044323.
4. *Zanotti E., Bisenberger M., Hertenberger R. et al.* Q3D focal plane detector at Munich Tandem // Nucl. Instrum. Methods. - 1991. - Vol. A310, Issue 2. - P. 706 - 712.
5. *Wirth H.-F.* New Q3D focal plane detector with cathode-strip readout. - Ph. D. thesis, Techn. Univ. München, 2001.
6. *Riess F.* GASPAN at the UNIX computers. Beschleunigerlaboratorium München // Annual Report, 1991. - P. 168.
7. *Akovali Y. A.* Nucl. Data Sheet for A = 230 // NDS. - 1993. - Vol. 69, Issue 1. - P. 155 - 208.
8. *Ackermann B., Baltzer H., Freitag K. et al.* Experimental Investigation of Vibrational Excitations in ^{230Th} // Z. Phys. - 1994. - Vol. A350. - P. 13.
9. *Kunz P. D.* Computer code CHUCK3. - University of Colorado, unpublished.
10. *Becchetti F. D., Greenlees G. W.* // Phys. Rev. - 1969. - Vol. 182. - P. 1190.
11. *Flynn E. R., Amstrong D. D., Beery J. G., Blair A. G.* Triton Elastic Scattering at 20 MeV // Phys. Rev. - 1969. - Vol. 182, Issue 4. - P. 1113 - 1120.
12. *Becchetti F. D., Greenlees G. W.* Proc. Third Int. Symp. on polarization phenomena in nuclear reactions (Medison, 1970) / Ed. H. H. Barshall, W. Haeberli. - Medison: University of Wisconsin Press, 1971. - P. 682.
13. *Ardisson G., Hussonnois M., LeDu J. F. et al.* Levels of ^{232}U fed in ^{236}Pu α decay // Phys. Rev. - 1994. - Vol. 49, Issue 6. - P. 2963 - 2970.
14. *Gerl J., Elze Th. W., Ower H. et al.* Electromagnetic properties of ^{230}Th studied by Coulomb excitation // Phys. Rev. - 1984. - Vol. 29, Issue 5. - P. 1684 - 1692.
15. *Kulessa R., Briancon Ch., Lefebvre A. et al.* Coulomb Excitation of ^{230}Th with ^{32}S, ^{84}Kr and ^{142}Nd Projectiles // Z. Phys. - 1989. - Vol. A334. - P. 299.

КОЛЕКТИВНІ СТАНИ В ^{230}Th: ЕКСПЕРИМЕНТАЛЬНІ ДАНІ

О. І. Левон, Г. Грав, І. Айзерман, Р. Гертенбергер, Р. Г. Тірольф, Г.-Ф. Вірс

Спектри збудження в деформованому ядрі ^{230}Th досліджено в (p, t)-реакції, використовуючи Q3D-спектрограф на Мюнхенському тандем-прискорювачі. Кутові розподіли тритонів одержано для 200 збуджених станів для енергій до 3,3 МеВ включно. З порівняння експериментальних кутових розподілів із розрахованими, користуючись наближенням зв'язаних каналів (код CHUCK3), визначено спіни збуджених станів до 6^+. Спіни 0^+ надійно визначено для 16 станів, відносно надійно – для 4 станів. Аналіз одержаних даних буде викладено в наступній статті.

Ключові слова: (p, t)-спектроскопія, Q3D-спектрограф, кутові розподіли, аналіз зв'язаних каналів, колективні стани.

КОЛЛЕКТИВНЫЕ СОСТОЯНИЯ В ^{230}Th: ЭКСПЕРИМЕНТАЛЬНЫЕ ДАННЫЕ

А. И. Левон, Г. Грав, И. Айзерман, Р. Гертенбергер, Р. Г. Тирольф, Г.-Ф. Вирс[2]

Спектры возбуждения в деформированном ядре ^{230}Th исследованы в (p, t)-реакции, используя Q3D-спектрограф на Мюнхенском тандем-ускорителе. Угловые распределения тритонов измерены для 200 возбужденных состояний для энергий до 3,3 МэВ включительно. Из сравнения экспериментальных угловых распределений с вычисленными, используя приближение связанных каналов (код CHUCK3), определены спины возбужденных состояний вплоть до 6^+. Спины 0^+ надежно определены для 16 состояний, относительно надежно – для 4 состояний. Анализ полученных данных будет изложен в следующей статье.

Ключевые слова: (p, t)-спектроскопия, Q3D-спектрограф, угловые распределения, анализ связанных каналов, коллективные состояния.

Received 14.07.09,
revised - 12.11.09.